Notch3 signaling gates cell cycle entry and limits neural stem cell amplification in the adult pallium

Alessandro Alunni, Monika Krecsmarik, Adriana Bosco, Sonya Galant, Luyuan Pan, Cecilia B Moens, Laure Bally-Cuif

Development 140, 3335-3347 (2013) doi:10.1242/dev.095018

Notch3 signaling gates cell cycle entry and limits neural stem cell amplification in the adult pallium

Alessandro Alunni[1,*,‡], Monika Krecsmarik[1,*], Adriana Bosco[1], Sonya Galant[1], Luyuan Pan[2], Cecilia B. Moens[2] and Laure Bally-Cuif[1,‡]

SUMMARY

Maintaining the homeostasis of germinal zones in adult organs is a fundamental but mechanistically poorly understood process. In particular, what controls stem cell activation remains unclear. We have previously shown that Notch signaling limits neural stem cell (NSC) proliferation in the adult zebrafish pallium. Combining pharmacological and genetic manipulations, we demonstrate here that long-term Notch invalidation primarily induces NSC amplification through their activation from quiescence and increased occurrence of symmetric divisions. Expression analyses, morpholino-mediated invalidation and the generation of a *notch3*-null mutant directly implicate Notch3 in these effects. By contrast, abrogation of *notch1b* function results in the generation of neurons at the expense of the activated NSC state. Together, our results support a differential involvement of Notch receptors along the successive steps of NSC recruitment. They implicate Notch3 at the top of this hierarchy to gate NSC activation and amplification, protecting the homeostasis of adult NSC reservoirs under physiological conditions.

KEY WORDS: Notch3, Adult neural stem cell, Quiescence

INTRODUCTION

Constitutive tissue renewal is controlled by the activity of stem cells, long-lasting progenitors with the potential for self-renewal and multipotency, which coordinate the generation of differentiated progeny with the maintenance of stem cell pools (germinal zones, GZs). Germinal pools homeostasis should avoid both depletion and uncontrolled amplification. Several cellular parameters impact on this process, which includes the maintenance of stem cell 'stemness' and of the speed and mode of stem cell divisions. The mechanisms coordinating the maintenance, loss or amplification of individual stem cells and the frequency of stem cell divisions to preserve the overall size of germinal pools are only beginning to be unraveled.

In the adult mammalian brain, the major constitutively active neurogenic zones are the subependymal zone (SEZ) of the telencephalic lateral ventricle and the subgranular zone (SGZ) of the dentate gyrus in the hippocampus (Doetsch et al., 1999; Seri et al., 2001). The prevailing model in both domains proposes that neural stem cells (NSCs) display astroglial characteristics, are essentially quiescent and generate transit amplifying progenitors (TAPs) through asymmetrical divisions (Kriegstein and Alvarez-Buylla, 2009). Symmetric divisions of astroglial progenitors, presumably increasing the NSC pool, have been reported *in vitro* (Costa et al., 2011) and in rare instances *in vivo* (Suh et al., 2007), as well as cases for direct NSC differentiation (Bonaguidi et al., 2011; Encinas et al., 2011), suggesting that maintenance of the SEZ/SGZ must accommodate events of NSC amplification and loss. Several signaling pathways, including Notch (Ables et al., 2011; Imayoshi et al., 2010; Pierfelice et al., 2011) and PEDF (Andreu-Agulló et al., 2009), preserve stemness and may impact on NSC maintenance and the outcome of stem cell divisions.

Much less is known about the processes controlling NSC activation, the rate of NSC divisions *in vivo*, and the impact of NSC division frequency on NSC maintenance. The local NSC microenvironment, as well as BMP and Notch, have been implicated in the control of NSC activation in the adult mouse (Kazanis et al., 2010; Mira et al., 2010; Ehm et al., 2010). One study reports that abrogating canonical Notch signaling in adult NSCs of the SGZ results in a transient burst of NSC proliferation, suggesting a role for this pathway in inhibiting NSC activation and/or proliferation (Ehm et al., 2010). However, in apparent contrast with this interpretation, most analyses in the adult SEZ and SGZ highlight that Notch invalidation is followed by NSC depletion (Ables et al., 2010; Ehm et al., 2010; Imayoshi et al., 2010). Unlike the limited neurogenesis of the mammalian brain, adult neurogenesis is extremely pronounced in teleost fish, where new neurons are generated in most brain regions during adult life. This is accompanied by the maintenance of long-lasting progenitors in a high number of constitutively active germinal niches (Lindsey and Tropepe, 2006; Chapouton et al., 2007; Kaslin et al., 2008). In the dorsal telencephalon (pallium), the majority of progenitor cells along the neurogenic ventricular zone are radial glia (RG) (Chapouton et al., 2010; März et al., 2010; Ganz et al., 2010), and single-cell tracing has identified precursors with NSC properties within this population (Rothenaigner et al., 2011). In contrast to mouse, asymmetrical NSC divisions in this system (which generate a RG and an intermediate neuronal precursor) are in the minority; rather, pallial RG mostly undergo symmetric divisions, amplifying the NSC pool (Rothenaigner et al., 2011). Overall, however, as in mouse, RG are strongly quiescent (Chapouton et al., 2010; März et al., 2010; Rothenaigner et al., 2011), and we recently observed that blocking Notch signaling for 2 days increased the RG population in proliferation (Chapouton et al., 2010), suggesting an effect of Notch on NSC proliferation kinetics. These parallel and complementary studies open the possibility that Notch may control NSC activation.

Notch receptors (Notch1-Notch4 in mouse; Notch1a/b, Notch2 and Notch3 in zebrafish) are transmembrane proteins activated by

[1]Institute of Neurobiology A. Fessard, Laboratory of Neurobiology and Development, CNRS UPR3294, Team Zebrafish Neurogenetics, Avenue de la Terrasse, Building 5, F-91198 Gif-sur-Yvette, France. [2]Division of Basic Sciences, Fred Hutchinson Cancer Research Center, B2-152, 1100 Fairview Avenue North, Seattle, WA 98109, USA.

*These authors contributed equally to this work
‡Author for correspondence (alunni@inaf.cnrs-gif.fr; bally-cuif@inaf.cnrs-gif.fr)

Accepted 10 June 2013

Delta and Jagged ligands (in vertebrates) and involved in a number of cell fate decisions in various tissues, including the nervous system (Yoon and Gaiano, 2005; Louvi and Artavanis-Tsakonas, 2006). Upon activation, the intracellular domain of Notch (NICD) is cleaved by the γ-secretase complex and translocates into the nucleus where it associates with the co-activator Mastermind and activates the transcriptional regulator RBPJk (Suppressor of Hairless [Su(H)], CSL) to trigger the transcription of target genes (notably *Hes*/*her* genes in mouse and zebrafish, respectively). In the nervous system, Notch activation classically inhibits neuronal differentiation (reviewed by Pierfelice et al., 2011). Notch activity, revealed by immunocytochemistry or reporter transgenes, was generally mapped to GFAP-positive or Sox2-positive NSCs, both in the SEZ and SGZ and in TAPs (Breunig et al., 2007; Ehm et al., 2010; Lugert et al., 2010; Imayoshi et al., 2010). Likewise, *notch* and *her* genes are strongly expressed in quiescent RG of the adult zebrafish pallium (Chapouton et al., 2010; Chapouton et al., 2011; Ganz et al., 2010). Here, we use this experimental system to demonstrate for the first time that Notch3 activity gates NSC activation, thereby ensuring GZ homeostasis. This function appears strikingly different from the role of Notch1b, which prevents the differentiation of activated progenitors. These data together place different Notch receptors along the successive steps of NSC recruitment.

MATERIALS AND METHODS

Zebrafish and *in vivo* manipulations

All experiments on animals conform to the official regulatory standards of the Department of Essonne (agreement number A 91-577 to L.B.C.). Three- to 9-month-old or juveniles of the wild-type AB zebrafish strain, the transgenic line *Tg(gfap:gfp)*^{mi2001} (Bernardos and Raymond, 2006) (referred to as *gfap:gfp*) and the *notch3*^{fh332} mutant allele (see below) were used. To apply one thymidine analogue, the fish were kept in tank water with 1 mM IdU, CldU or BrdU for 6 hours. To apply multiple analogues, the fish were anesthetized in 0.02% tricaine and equimolar concentrations of BrdU and EdU (10 mM) were injected intraperitoneally (0.5 µl/0.1 g body weight). Five days post-fertilization (dpf) or 7 dpf juveniles were soaked in 10 mM BrdU, 15% DMSO in embryo medium (EM) for 20 minutes on ice then washed in EM. Notch signaling was blocked using 10 µM LY411575 (wt/vol) (Fauq et al., 2007) in the swimming water at 28°C. The LY solution was exchanged daily for treatments of less than 7 days, or every week for longer treatments (supplementary material Fig. S3), with no loss of efficiency (not shown). Control fish were treated with the same final concentration (0.04%) of DMSO carrier.

To selectively block either Notch3 or Notch1b functions, we electroporated fluorescein-tagged splice *notch3* or *notch1b* morpholinos (MOs) (GeneTools, Philomath, OR, USA) into neural progenitors of the adult pallium: MOs at 1.2 mM were injected into the brain ventricle of anesthetized adults as described previously (Rothenaigner et al., 2011) and two pulses (70 V, 50 mseconds) were applied using an Intracel TSS20 ovodyne electroporator with an EP21 current amplifier between electrodes placed above and below the fish head. The MOs used (*notch3*-MO, 5′AAGGATCAGTCATCTTACCTTCGCT3′; *notch1b*-MO, 5′AATCTC-AAACTGACCTCAAACCGAC3′) were previously validated (Ma and Jiang, 2007; Milan et al., 2006). Electroporation of a generic fluorescein-tagged MO was used as control (control-MO: 5′CCTCTTACCT-CAGTTACAATTTATA 3′).

Generation and identification of the notch3^{fh332} allele

We used the TILLING method (Draper et al., 2004) to identify an ENU-induced nonsense mutation in *notch3*, as described at http://labs.fhcrc.org/moens/Tilling_Mutants/notch3/allele_1.html. For genotyping, PCR was performed from genomic DNA using the following primers: forward, 5′CCCTGAAGGGTTCCATGATCCCTACTACTA3′; reverse, 5′TCCA-GGCTCACAGTCACACCGATA3′. The PCR products were digested with *Spe*I, generating a shorter band in mutants (182 bp instead of 212 bp).

Immunohistochemistry

For analyses of adult brains, the following primary antibodies were applied onto free-floating 50 µm vibratome sections: GFP (1:500, Aves Laboratories), MCM5 (1:500, kindly provided by Soojin Ryu, Max Planck Institute for Medical Research, Heidelberg, Germany), HuC/D (1:600, mouse, Invitrogen; 1:2000, human, a gift from Dr B. Zalc, Salpêtrière Hospital, Paris), BrdU (1:1000, mouse clone MoBU-1, Invitrogen; 1:250, rat, Abcam), glutamine-synthase (1:500, mouse, Millipore) and S100β (1:1000, rabbit, Dako). For BrdU, IdU and CldU detection, sections were incubated in 2 M HCl for 30 minutes at 37°C. To detect EdU, we used the Click-iT Imaging Kit (Invitrogen). Secondary antibodies raised in goat coupled to AlexaFluor dyes (Invitrogen) were used (1:1000). For analyses of juveniles, cryosectioned brains were processed for immunohistochemistry with the antibodies above and, in addition, with anti-BLBP (rabbit, 1:500, Millipore) and anti-proliferating cell nuclear antigen (mouse anti-PCNA, 1:250, Santa Cruz Biotechnology).

In situ hybridization

Whole dissected adult brains were incubated at 65°C for 18 hours in 2 ng/µl DIG- and fluorescein-labeled mRNA probes for *notch3*, *notch1b*, *jagged1a*, *jagged1b* and *jagged2* (plasmids provided by Julian Lewis's lab, London Research Institute, UK) and in DIG-labeled *deltaA*, *deltaB* and *deltaD* probes (provided by Bruce Appel, University of Colorado, Aurora, CO, USA). Next, cross-sections were vibratome cut and incubated with anti-DIG POD (sheep, Roche, 1:500) or anti-Fluo POD (sheep, Roche, 1:500). The signal was revealed using home-made FITC and Cy3-conjugated tyramide (http://www.xenbase.org/other/static/methods/FISH.jsp). For single stainings, the sections were incubated with anti-DIG AP Fab fragments (sheep, Roche, 1:5000) and revealed with SIGMAFAST Fast Red/TR Naphthol (Sigma).

Dissected juvenile brains were hybridized with a DIG-labeled probe, then cryosectioned, incubated with anti-DIG-AP Fab fragments (Roche) and processed with Fast Red.

Image acquisition and cell counting

All images were taken on a Zeiss LSM700 confocal microscope using 20× air, 40× oil or 63× oil objectives. Images were processed using the ZEN software (Zeiss). Measurements (supplementary material Fig. S3) were acquired using ImageJ. For cell countings in Figs 1, 2 and 5, counting was carried out manually on *z*-stacks from 50 µm serial sections from four telencephali for each condition. For Fig. 7, three non-consecutive sections per juvenile brain and a minimum of five brains per experiment were counted.

Statistics

All experimental data are expressed as mean±s.e.m. The data obtained were compared using unpaired two-sided Student's *t*-test, Fisher's exact test when comparing two groups and one-way ANOVA followed by Bonferroni *post hoc* test when comparing more than two groups. Significance was set at $P<0.05$. Data were analyzed using Excel software and Statistica.

RESULTS

Notch invalidation recruits quiescent RG into amplifying gliogenic divisions

To assess the effect of canonical Notch signaling on RG proliferation, we blocked Notch using the γ-secretase inhibitor LY411575 (referred to as LY) (Rothenaigner et al., 2011; Ninov et al., 2012) applied to *gfap:gfp* transgenic fish (Bernardos and Raymond, 2006), where GFP faithfully labels pallial RG (Chapouton et al., 2010). The resulting proliferation phenotype reads out a specific effect of γ-secretase inhibitors on Notch signaling (Chapouton et al., 2010). This treatment also leads to a massive downregulation of the *her* gene *her4.1* expression in RG (supplementary material Fig. S1A,B), confirming that *her4.1* is a Notch target in this system, as in the embryo (Takke et al., 1999).

Notch inhibition for 2 days increases the proportion of dividing RG within the pallial germinal pool (Chapouton et al., 2010). This

could result from accelerating the divisions of RG that were already in proliferation at the time of treatment (Notch acting on cell division speed), from recruiting quiescent RG into the cell cycle (Notch acting on RG activation), or from both. To determine the relative contribution of initially cycling and quiescent RG to the effect of Notch blockade, we administered to adult zebrafish a single pulse of the thymidine analog EdU to label a cohort of RG in S phase. We subsequently blocked Notch and applied a second pulse with the analog BrdU to mark RG cells that are dividing during Notch blockade (Fig. 1A). The time between the EdU pulse and the LY treatment was chosen as being sufficient to allow most EdU-labeled RG to terminate their cell cycle before the onset of Notch blockade (not shown). A triple immunolabeling was then used to quantify EdU-positive, BrdU-positive and EdU/BrdU double-labeled cells within the RG (GFP-positive) population (Fig. 1B,C). Strikingly, we observed that the number of EdU-positive RG per section, whether labeled with EdU only or with EdU and BrdU, was not significantly different under control and LY-treated conditions (Fig. 1C, blue and purple bars). There was a trend decrease for EdU only-positive cells; however, this did not reach significance. In sharp contrast, the number of RG that entered S phase during Notch blockade and were only BrdU-positive was significantly increased compared with control conditions (Fig. 1C, red bars). Thus, Notch blockade induces quiescent RG to enter the cell cycle and has no significant effect on cell cycle re-entry in previously dividing RG.

Adult zebrafish pallial progenitors can undergo symmetric gliogenic divisions generating two RG, symmetric neurogenic divisions that generate two neuronal precursors (non-RG progenitors) and asymmetric divisions generating one RG and a neuronal precursor (Rothenaigner et al., 2011). Our previous clonal analyses showed that Notch blockade increased the number of all division events, but did not modify their relative proportions (Rothenaigner et al., 2011). However, the analysis time point took place long after cell labeling (4 weeks) and followed a 2-day LY treatment. Hence, we could not distinguish the primary and secondary effects of Notch blockade on cell division modes that may be consecutive during lineage progression. To address this issue, we used the experimental paradigm in Fig. 1A and counted BrdU-positive (Notch-induced) cell doublets at the end of the LY treatments (i.e. 1 day after BrdU labeling) to highlight the

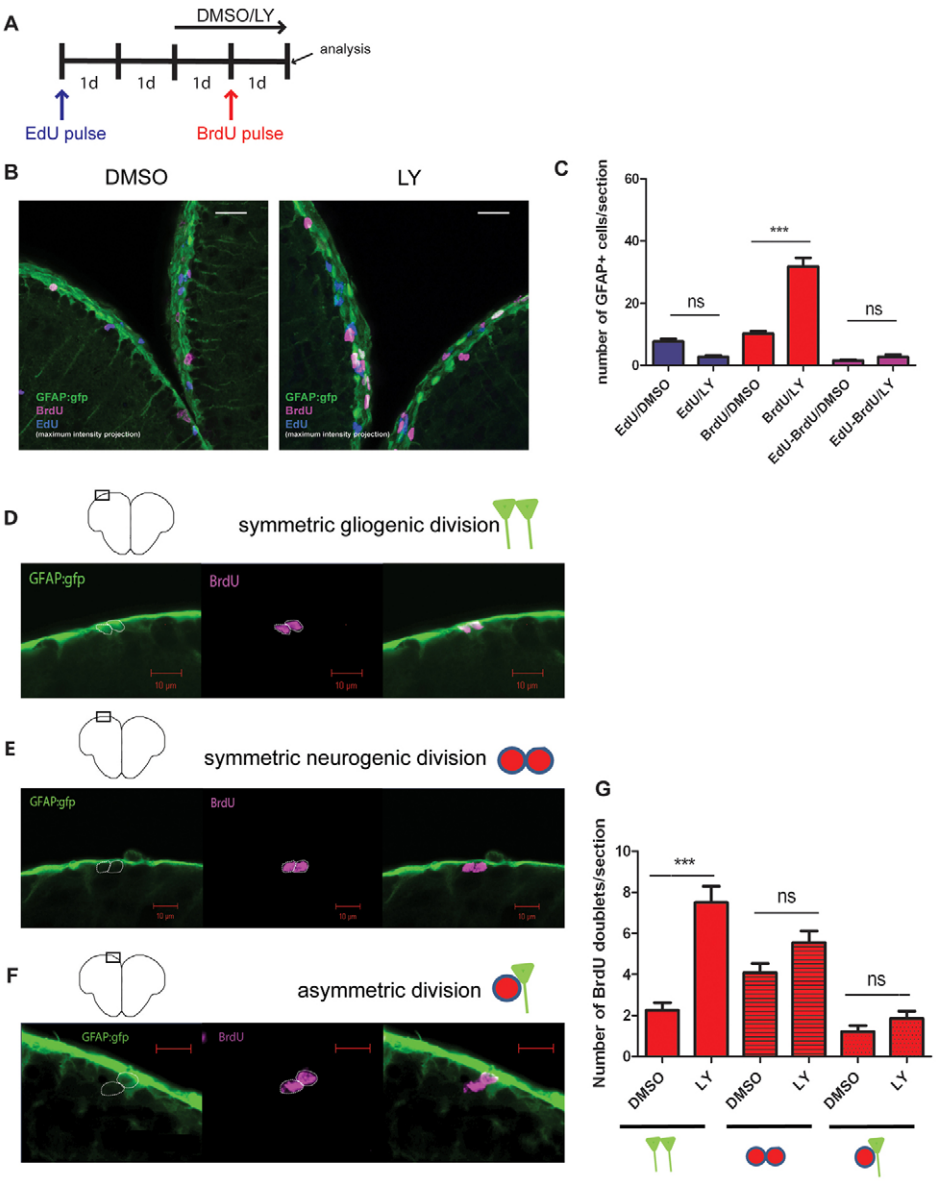

Fig. 1. Symmetrically dividing radial glial cells (RG) are recruited into the cell cycle during Notch blockade. (**A**) Experimental design. An initial cohort of RG in S phase was labeled with an EdU pulse followed by a second pulse of BrdU during Notch blockade (LY). 1d, 1-day intervals. (**B**) Triple immunostaining showing GFAP- (green), BrdU- (magenta) and EdU- (blue) positive cells in the Dm region of the pallium (confocal projections over 16 and 19 µm, respectively). (**C**) Quantification of EdU-positive, BrdU-positive and EdU/BrdU-positive RG. Red bars, $P<0.0001$; blue bars, $P=0.07$; pink bars, $P>1$ ($n=4$ brains for each treatment, total number of cells counted: 1156). (**D-G**) Division modes of RG and quantification of BrdU-positive doublets in the experimental setting shown in A. Symmetric gliogenic divisions, $P<0.0001$; other division modes, $P>1$; $n=273$ doublets counted. Scale bars: white, 20 µm; red 10 µm.

immediate effect of Notch blockade. Quantified doublets, corresponding to sister cells following M phase, were defined as adjacent cells co-labeled with BrdU and distant from the next identically labeled ventricular cells by at least four cell diameters (25 μm). We observed a significant increase in the number of symmetric gliogenic divisions (Fig. 1D,G), but not of other division modes (Fig. 1E-G), for the cells newly dividing during Notch blockade. We conclude that the RG cells recruited into cycle by Notch blockade primarily undergo symmetric gliogenic divisions. Thus, Notch signaling inhibits RG activation and specifically limits their amplifying divisions.

Notch invalidation triggers overgrowth of the pallial GZ through a rapid amplification of the RG population

Notch blockade for 2 days leads to the expression of proliferation markers in 60% of RG (Chapouton et al., 2010). It remains unclear whether this proportion reveals a cryptic heterogeneity within the RG population, with competent versus incompetent RG in the face of Notch blockade. In addition, whether RG activation is transient and followed or attenuated by NSC depletion, resembling the effect of Notch blockade in mouse (Ables et al., 2010; Ehm et al., 2010; Imayoshi et al., 2010), is unknown. To study these aspects, we examined the effect of longer Notch invalidations.

In control fish, 15% of RG express proliferation markers such as mini-chromosome maintenance 5 (MCM5) (Ryu et al., 2005) (Fig. 2A,F), in agreement with previous reports (Chapouton et al., 2010; März et al., 2010). We verified that blocking Notch for 2 days led to the activation of MCM5 expression in 60% of RG (Fig. 2B,F). After 3 days of treatment, virtually all RG were proliferating (95% of MCM5-positive RG) (Fig. 2C,F), and this proportion remained at this highest level after 5 and 7 days of treatment (Fig. 2D-F). Thus, virtually all RG are capable of responding to Notch blockade within 3 days, although some show a delay in their activation.

We noticed the appearance of several RG layers along the pallial ventricular zone after a few days of LY treatment (Fig. 2D,E),

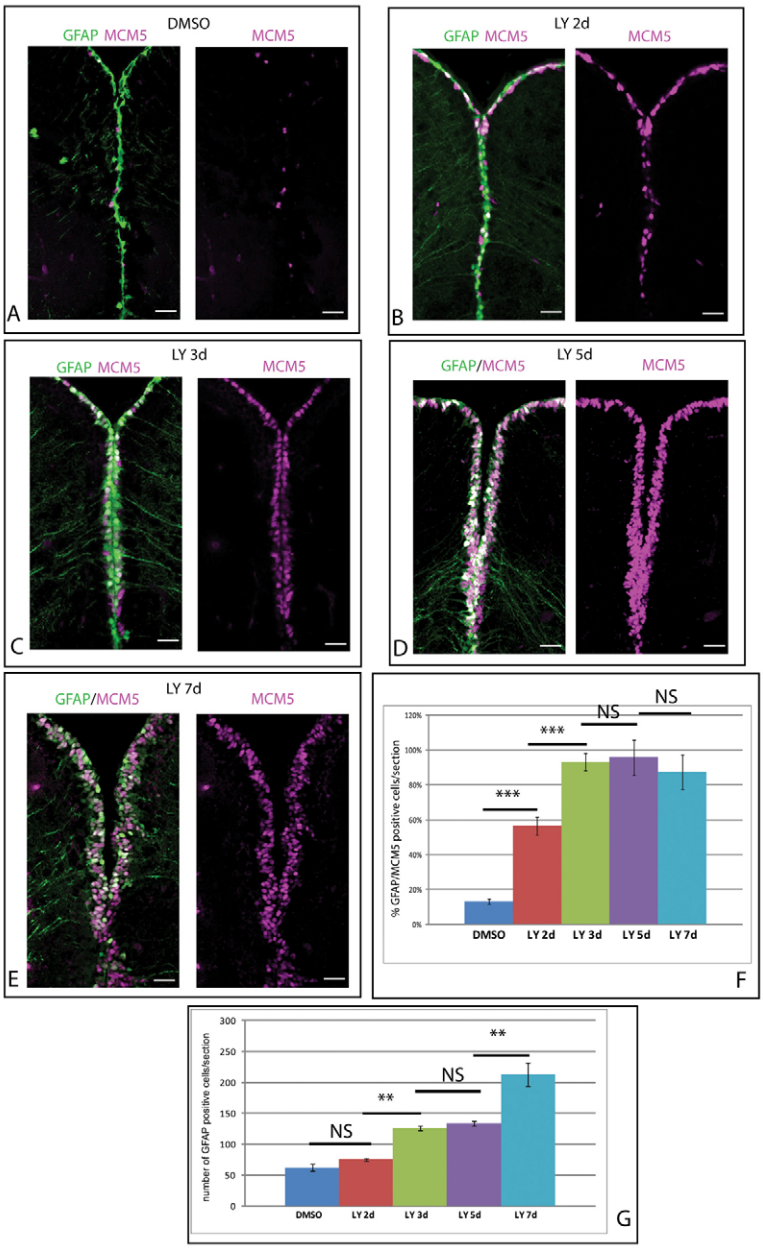

Fig. 2. Notch invalidation triggers continuous overgrowth of the pallial GZ through RG amplification. (**A-E**) Cross-sections of the pallial ventricular zone following different length of LY411575 treatment (d, days of treatment) stained for the RG marker GFAP-GFP (green) and the proliferation marker MCM5 (magenta). (**F**) Percentage of RG in cycle (GFAP/MCM5 positive) during LY treatment. (**G**) Total number of RG (GFAP positive). ***P*<0.005; ****P*<0.0001 (*n*=4 brains for each condition). Scale bars: 20 μm. Confocal projections of four optical planes (each 1 μm).

suggesting that the increased proportion of MCM5-positive RG may be accompanied with an enlargement of the RG population. To validate this observation, we quantified GFAP-positive cells over time. During the first 2 days, the total number of RG cells per section remained at its initial value, but this number then doubled twice through the duration of treatment, between days 2 and 3, then days 5 and 7 (Fig. 2G). These findings suggests that two distinct phases of response take place upon long-term Notch invalidation: recruitment of the full RG population into cycle during the first 3 days, and successive division events that amplify the RG pool from day 2 onwards. At this point, all RG remain MCM5 positive (Fig. 2E,F), suggesting that they do not reenter quiescence and are prone to dividing again. Confirming this point, the dividing status of reactivated RG appeared stable until at least 3 days following the arrest of treatment (supplementary material Fig. S2).

To challenge the limits of this amplification, we increased the duration of LY treatments for up to 5 weeks (supplementary material Fig. S3). Although we observed that the number of RG was still massively enlarged after a 3-week LY treatment, this was less prominent than with shorter durations (Fig. 2G) and tended to normalize after 5 weeks (supplementary material Fig. S3I). However, in striking contrast to control fish, RG maintained a stably increased proliferation rate even after 5 weeks of continuous Notch blockade (supplementary material Fig. S3J). Interestingly, these long-term modifications of RG activity did not impact the length of the pallial ventricular zone, but were paralleled by an obvious enlargement of the subventricular HuC/D-positive domain (supplementary material Fig. S3K,L). These observations highlight some level of regulation in RG amplification upon long-term Notch blockade, whereby a large proportion of amplified RG eventually generate a bulk of newborn neurons. However, an activated RG layer is maintained in a ventricular location, resembling the normal NSC pool except for its lack of quiescence.

Amplified RG display NSC properties at the single cell level

To first determine whether the LY-amplified RG population had maintained NSC properties, we analyzed its capacity for self-renewal and multipotentiality. Using a 7-day treatment paradigm, we marked proliferative cells 48 hours after the onset of Notch invalidation using CldU (supplementary material Fig. S4A). At this time point, 90% of the CldU-labeled population consists of RG recruited into the cell cycle as a result of Notch blockade (not shown). At the end of the 7-day LY treatment, 15% of CldU-labeled cells were still proliferating RG (white arrows in supplementary material Fig. S4B), illustrating self-renewal of the dividing RG status. Three days after the end of treatment, these cells had generated both non-dividing glia and differentiated neurons (supplementary material Fig. S4C,D). Thus, the population of RG cells recruited into the cell cycle upon Notch blockade also retains bipotent properties after long-term Notch invalidation.

To further investigate whether single RG from the amplified pool behave as NSCs, we used CldU-mediated tracing to track the fate of sister cells originating from RG divisions. CldU was applied 2 days after the end of a 7-day LY treatment (a stage when virtually all labeled cells belong to the amplified RG pool, not shown and see supplementary material Fig. S2), and the identity of CldU cell doublets was monitored after a 2-day chase (Fig. 3A). Along the ventricular zone of LY-treated fish, we observed symmetrical CldU cell doublets positive for glial markers, attesting to the occurrence of self-renewing symmetric gliogenic divisions (Fig. 3B-F), as well as asymmetrical doublets where one cell expressed a glial marker

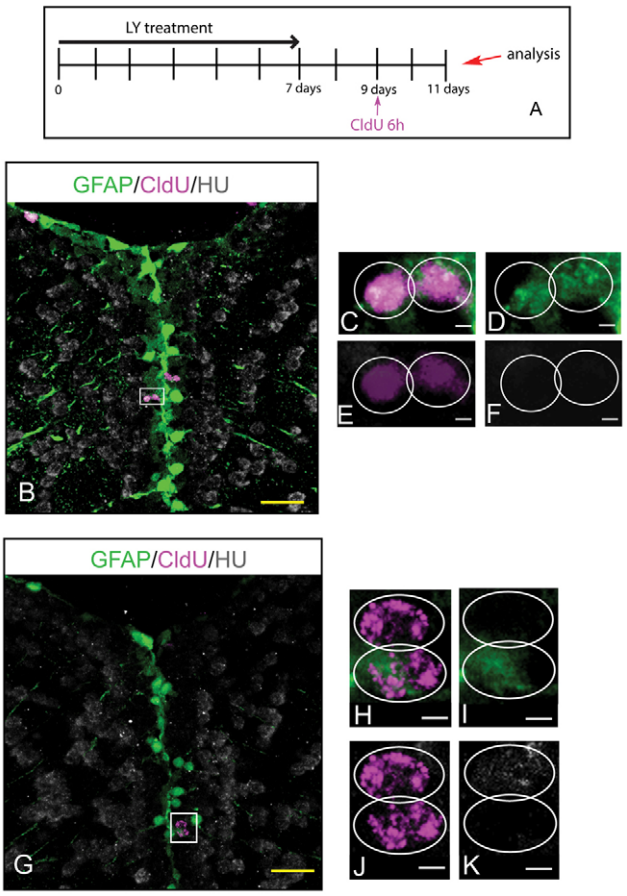

Fig. 3. Individual RG cells maintain stem cell properties after Notch blockade. (**A**) Experimental design. (**B-K**) Single optical section of the pallial ventricular zone in *gfap:gfp* transgenic brains, triple labeled for GFP (RG, green), CldU (magenta) and HuC/D (gray). (C-F) High magnification of the area boxed in B; example of a self-renewing, symmetric gliogenic division. (H-K) High magnification of the area boxed in G; example of a self-renewing and asymmetric division. Scale bars: yellow, 20 µm; white, 2 µm.

and the other a neuronal marker (Fig. 3G-K), highlighting bi-potentiality at the single cell level. These results indicate that RG from the amplified pool retain NSC properties at the single cell level, demonstrating that long-term Notch invalidation results in an expansion of the pallial germinal pool, with maintenance of NSC characteristics, except for a lack of quiescence.

These observations suggest that the activated RG state could be reversible when Notch levels are restored, with a rescue of GZ size and properties. To verify this, we analyzed the pallial ventricular zone in adult animals 1 month after the interruption of a 10-day Notch blockade. GZ morphology, RG numbers and the proportion of proliferating RG were indistinguishable from control fish (supplementary material Fig. S5). We conclude that a 10-day long Notch invalidation does not deplete NSCs in the zebrafish adult pallial GZ.

notch3 expression, but not *notch1*, characterizes adult pallial RG

Several *notch* receptors are expressed along the GZ of the adult zebrafish pallium (Chapouton et al., 2010). To identify the Notch receptors controlling the RG quiescence/activation cycle, we

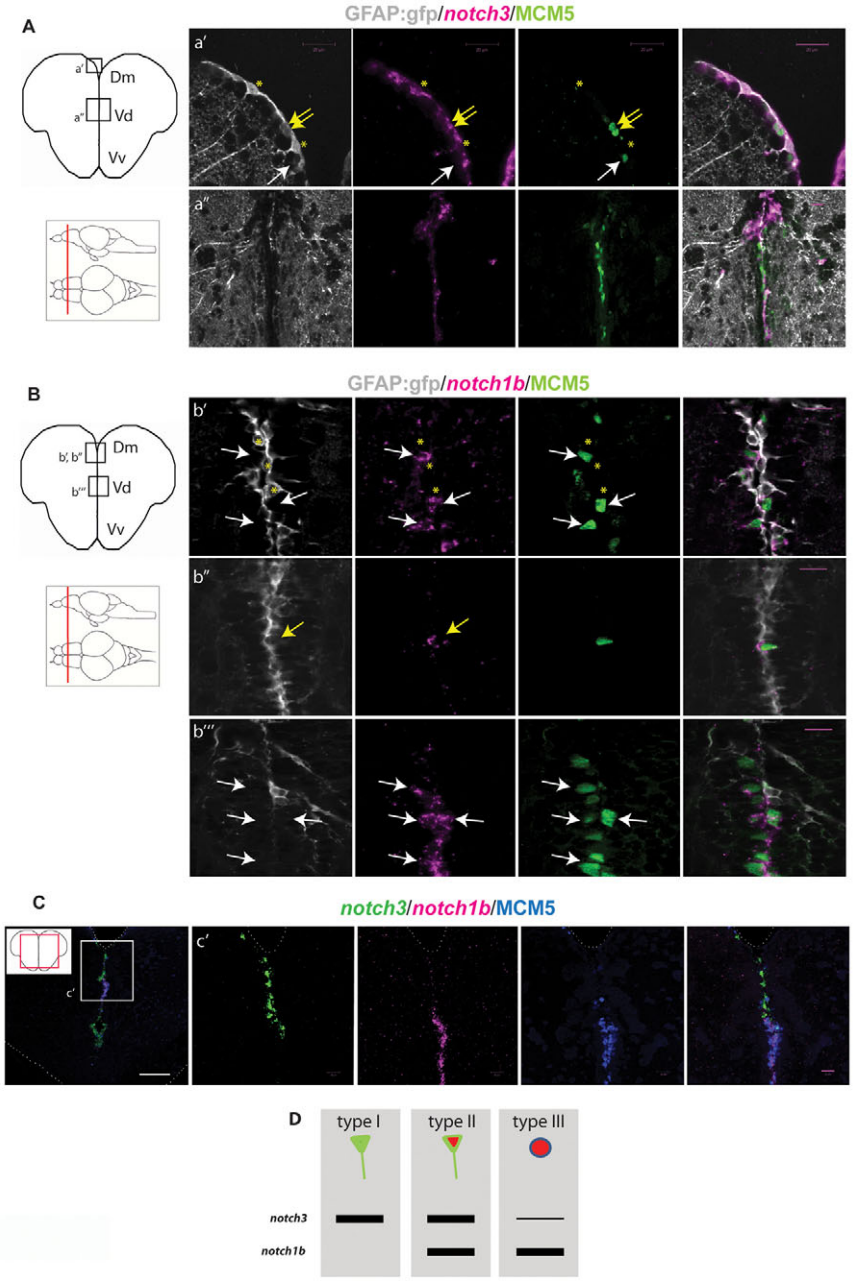

Fig. 4. *notch3* and *notch1b* are differentially expressed in adult pallial progenitors. (**A**) *notch3* expression revealed by fluorescent *in situ* hybridization (magenta) on telencephalic cross-sections of a *gfap:gfp* brain, together with a double fluorescent immunostaining for GFP (RG, gray) and MCM5 (green). (a′) Dorsomedial (Dm) region of the pallium, *notch3* expression is found in quiescent (type I) (yellow asterisks) and proliferating (type II) (yellow arrows) RG. Transcripts are absent from type III cells (white arrows). (a″) Pallial-subpallial junction, enriched in type III cells: *notch3* expression is very low or absent. (**B**) *notch1b* expression (magenta) compared with GFAP-GFP (RG, gray) and MCM5 (green). (b′,b″) Dm; white and yellow arrows indicate *notch1b*-positive type II RG (b′) and type III progenitors (b″), respectively. Transcripts are absent from quiescent RG (b′, yellow asterisks). (b‴) Pallial-subpallial junction: *notch1b* is strongly expressed in type III cells. (**C**) Double fluorescent *in situ* hybridization for *notch3* (green) and *notch1b* (magenta) with immunostaining for MCM5 (blue). (c′) High magnification of the pallial-subpallial junction: *notch3* is expressed by RG cells of Dm and *notch1b* by type III progenitors. (**D**) Graphic representation of *notch3* and *notch1b* expression in the different progenitor cell types (according to März et al., 2010). In Dm, *notch3* is expressed by 97% of type I cells (*n*=229 cells counted), 88% of type II cells (*n*=31 cells) and 2% of type III cells(*n*=23 cells); *notch1b* is expressed by 2.8% of type I cells (*n*=141 cells), 90% of type II cells (*n*=43 cells) and 85% of type III cells. Scale bars: white, 100 μm; magenta, 20 μm. Single optical confocal planes, 1 μm.

carefully analyzed the expression of *notch* genes in comparison with RG and proliferation markers (Fig. 4). Quiescent and proliferating RG were defined as type I and II cells, respectively, while proliferating neuronal precursors are known as type III (März et al., 2010). The expression of *notch1a* appeared too weak to be reliably assigned to a specific cell type (not shown), and *notch2* expression was not detectable. However, we found that all RG cells strongly express *notch3* RNA, irrespective of their proliferation status, whereas *notch3* expression is mostly absent from type III cells (Fig. 4A). By contrast, the expression of *notch1b* characterizes MCM5-positive cells, whether these are RG (type II) or proliferating neuronal precursors (type III), but was absent from quiescent RG (Fig. 4B). The differential expression of *notch1b* and *notch3* is particularly obvious around the pallial-subpallial boundary, where RG and proliferating neuronal precursors are spatially segregated (Fig. 4C). These observations demonstrate largely complementary expression of the *notch1b* and *notch3* genes (Fig. 4D), and suggest that the control of RG activation may rely on Notch3. Along these lines, we found that the expression of the Notch target *her4.1* (supplementary material Fig. S1A,B) was largely characteristic of quiescent *notch3*-positive RG, although some activated and *her4.1*-positive RG could be seen (supplementary material Fig. S1C,D). Notch ligand expression distributed differentially within the GZ and immediately adjacent newborn neurons, possibly creating a local niche (supplementary material Figs S6, S7).

Notch3 activity gates neural stem cell activation in the adult pallium

To selectively analyze the impact of Notch3 signaling on NSC proliferation, we applied the TILLING strategy to generate a *notch3* mutant allele (Draper et al., 2004). We recovered *notch3*^{fh332}, which harbors a nonsense mutation that introduces a premature stop codon at amino acid position 669 within the 8th Notch3 EGF repeat. This

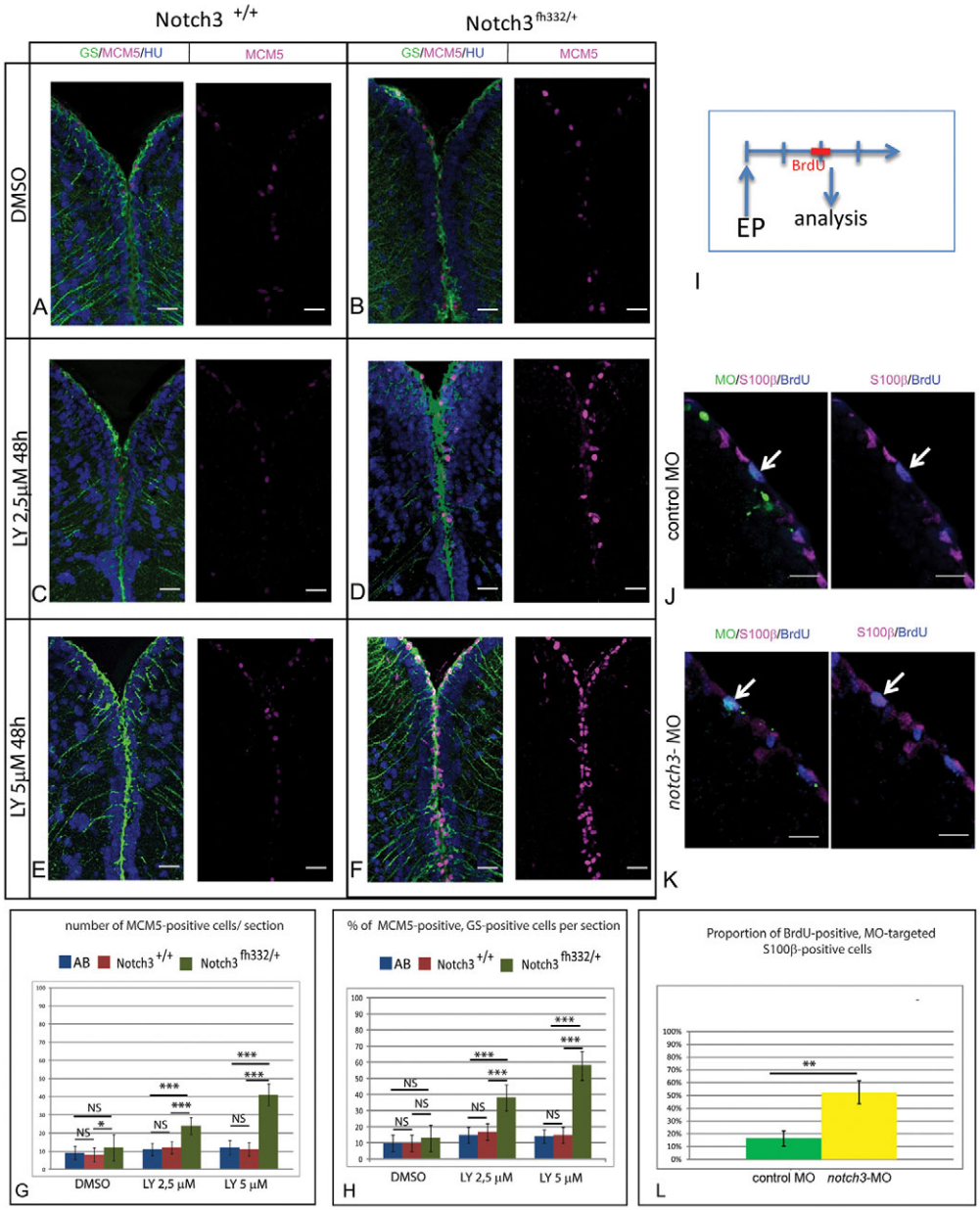

Fig. 5. Notch3 inhibition accounts for the effect of Notch blockade on RG activation. (**A-F**) Triple immunohistochemistry for the RG marker glutamine synthetase (GS, green), MCM5 (magenta) and HuC/D (blue) on telencephalic cross-sections from adult *notch3*$^{+/+}$ siblings and *notch3*$^{fh332/+}$ heterozygotes under control conditions (top row) or upon LY treatment (middle and bottom rows). Scale bar: 20 µm. Confocal projection images from four optical planes, each 1 µm thick. (**G**,**H**) Total number of MCM5-positive progenitors per section (G) and proportion of RG cells in proliferation (H) in the different genotypes and treatment conditions, as well as in the standard AB wild-type line. $P<0.0001$ ($n=3$ brains for AB, *notch3*$^{+/+}$ and *notch3*$^{fh332/+}$, respectively). (**I**) Schematic of the notch3-MO knock-down experiment: a BrdU pulse is applied 2 days after electroporation (EP) of fluorescein-labeled notch3-MO or control-MO in pallial ventricular cells. Brains are analyzed immediately. (**J**,**K**) Analysis of the proliferation status (anti-BrdU) (blue) of electroporated (fluorescein-positive) (green) RG (anti-S100β) (magenta), assessed by immunocytochemistry. Arrows indicate fluorescein-labeled radial glia BrdU-positive cells. Scale bar: 20 µm. Confocal projection images from four optical planes, each 1 µm thick. (**L**) Proportion of BrdU-positive cells within the radial glia MO-targeted population. $P<0.001$ ($n=3$ brains for each condition).

mutation is expected to generate a non-functional truncated protein lacking most of the extracellular and all of the transmembrane and intracellular domains of Notch3. *notch3*$^{fh332/fh332}$ homozygous embryos and larvae developed at normal speed and without apparent morphological defects (not shown), although the mutation was lethal before adulthood.

notch3$^{fh332/+}$ heterozygotes were adult viable and did not display any overt morphological or behavioral abnormality (not shown). At the cellular level in the pallium, their ventricular zone appeared largely indistinguishable from wild-type siblings or wild-type fish from the standard AB line, although the overall number of proliferating cells (MCM5-positive) was slightly but significantly increased over wild-type levels (Fig. 5A,B,G). However, the proportion of proliferating RG remained normal (Fig. 5H). As a first approach to assess the relevance of Notch3-mediated signaling in adult RG quiescence, we tested the sensitivity of adult *notch3*$^{fh332/+}$ heterozygotes to low doses of LY. We found that ventricular zone proliferation and the proportion of proliferating RG in the pallium were significantly and progressively increased in *notch3*$^{fh332/+}$ heterozygotes at doses that did not trigger any response in wild-type siblings or AB fish (Fig. 5A-H). Thus, decreased Notch3 signaling lowers the sensitivity threshold of RG to LY, indicating that Notch3 mediates at least part of the effect of Notch blockade on RG activation.

To further ascertain the role of Notch3 in limiting RG cycling, we blocked Notch3 function by electroporating a fluorescein-tagged splice morpholino (MO) targeting *notch3* (Ma and Jiang, 2007) into pallial ventricular progenitors in live fish. Forty-eight hours after electroporation, we assessed the activation status of RG by measuring BrdU incorporation in S100β-positive cells (Fig. 5I). The proportion of BrdU-positive RG was massively increased within the *notch3*-MO-electroporated (fluorescein-labeled) RG population compared with RG cells electroporated with a control MO (Fig. 5J-L). Furthermore, the activation value obtained (threefold) was in agreement with the response of RG to a 2-day LY treatment (see Fig. 2F). Together, we conclude that Notch3 signaling is limiting

activation of quiescent RG in the adult pallium and is the main target of LY inhibition in this cell population.

Notch3 activity limits RG activation towards amplifying divisions

To assess the effect of a complete genetic blockade of Notch3 on RG behavior, including division mode, we analyzed *notch3*$^{fh332/fh332}$ homozygous juveniles. The morphology of the juvenile telencephalon resembles that of the adult, with an externally located (‘everted’) ventricular zone (Folgueira et al., 2012) composed for a majority of RG, as revealed using the glial markers GS or BLBP (Figs 6, 7).

At developmental stages, pallial RG are actively proliferating (Dong et al., 2012). We found that, in the medial pallium, RG progressively exit the cell cycle starting at 5 dpf onwards, reaching around 25% of RG in quiescence (PCNA-negative) at 7 dpf (L. Dirian and I. Foucher, unpublished; see Fig. 7D,E). At these stages, *notch3* is normally strongly and specifically expressed in medially located pallial RG (Fig. 6A,B). By contrast, *notch1b* expression is barely detectable in RG and overall rather characterizes actively proliferating progenitors situated more ventrally (Fig. 6C,D). Finally, expression of the Notch target *her4.1* was decreased in RG from 5 dpf onwards in *notch3*$^{fh332/fh332}$ homozygous mutants (supplementary material Fig. S1E,F). These observations identify Notch3 as a major component of Notch signaling in pallial RG cells, and validate the loss-of-function character of *notch3*$^{fh332/fh332}$ mutants.

To test for a role of Notch3 on RG activation and/or proliferation, we analyzed the medial pallium of *notch3*$^{fh332/fh332}$ homozygotes at 5 and 7 dpf (Fig. 7A-D,F,G), a period that overlaps the onset of quiescence entry in a measurable proportion of pallial RG (Fig. 7E). The proportion of proliferating RG was significantly increased in *notch3*$^{fh332/fh332}$ homozygotes compared with wild-type siblings at 7 dpf (Fig. 7E): in mutants, this proportion remains close to 100%, indicating that RG fail to exit cycling or to maintain quiescence. In addition, the total number of RG was increased in *notch3*$^{fh332/fh332}$ homozygotes at both stages (Fig. 7F,G), suggesting that additional RG-generating divisions also take place in the mutant. These divisions probably increase between 5 and 7 dpf, when their impact becomes visible on the total number of proliferating progenitors (PCNA-positive) (Fig. 7G). Overall, this phenotype is strikingly reminiscent of that caused by Notch signaling abrogation in the adult pallium (Fig. 2). To verify whether it involved, as in adult RG, an increase in amplifying RG divisions, we used a BrdU pulse applied at 5 dpf followed by a 2-day chase to trace dividing RG cells in *notch3*$^{fh332/fh332}$ homozygotes until 7 dpf (Fig. 7H-M). A prior characterization of BrdU-labeled cells at the 5 dpf stage revealed a normal number of RG in S-phase in *notch3*$^{fh332/fh332}$ homozygotes (Fig. 7H,I,L). Following 2 days of chase, however, the number of BrdU-positive RG was significantly higher in mutants (Fig. 7J,K,M), demonstrating an increase in the number of RG-generating divisions at the ventricle. As the majority of BrdU-incorporating progenitors at 5 dpf are RG (Fig. 7L, compare BrdU with BrdU/BLBP), we conclude that the *notch3*$^{fh332/fh332}$ homozygous phenotype observed at 7 dpf results from an increased number of amplifying (symmetric) gliogenic divisions from 5 dpf onwards. Together, these results implicate Notch3 in driving RG quiescence to limit amplifying RG divisions.

Notch1b signaling is required to maintain activated progenitors in the adult pallial GZ

The expression of *notch1b*, which appeared specific of proliferating cells (states II and III), suggested a distinct function in adult progenitors compared with Notch3. To address this point, we repeated electroporation of fluorescein-labeled MOs into adult pallial progenitors in live fish, this time using a splice MO directed against *notch1b* (Milan et al., 2006). We found that blocking Notch1b activity did not affect the proportion of RG in cycle (MCM5-positive, GS-positive cells) 2 days after electroporation, but strongly decreased this proportion by 5 days (Fig. 8A-D). This decrease could result from the accelerated conversion of type II cells to quiescent glia after division, and/or to their loss of a RG identity. To sort out between these possibilities, we traced the fate of proliferating progenitors upon Notch1b blockade using a BrdU pulse-chase assay (Fig. 8E). Two days after electroporation, within the MO-targeted (fluorescein-positive) population, the proportion of RG cells in S phase (labeled with the BrdU pulse) was not affected upon electroporation of *notch1b*-MO (Fig. 8F-H). This is in agreement with MCM5 expression (Fig. 8D), indicating that

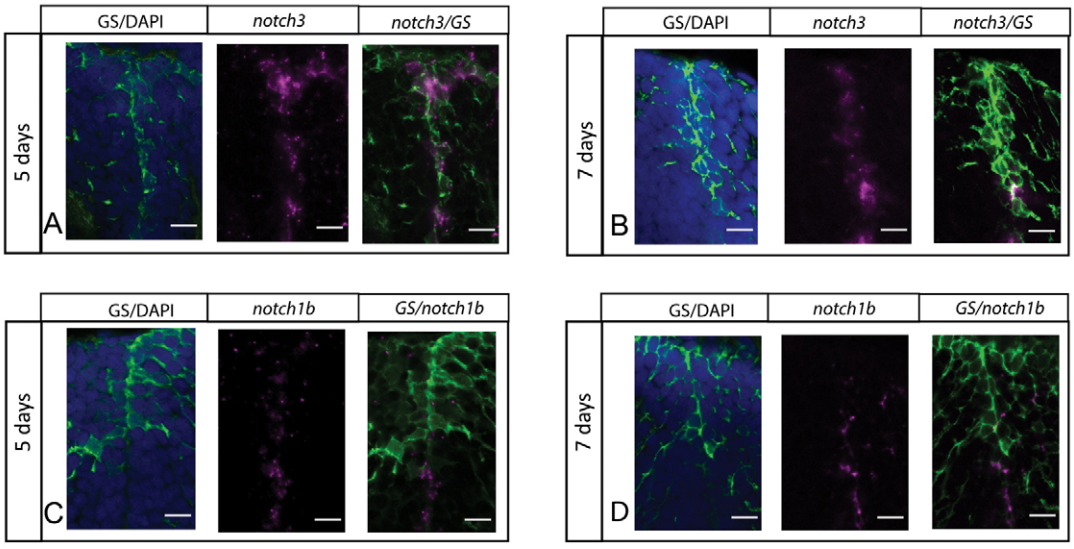

Fig. 6. *notch3* expression, but not *notch1b*, characterizes RG of the juvenile zebrafish pallium. (**A-D**) Fluorescent *in situ* hybridization (magenta) for *notch3* (A,B) or *notch1b* (C,D), and immunocytochemistry for the RG marker GS (green) (blue: DAPI), on cross-sections of the pallium at 5 and 7 dpf. Scale bars: 10 μm. Confocal projection images from four optical planes, each 1 μm thick.

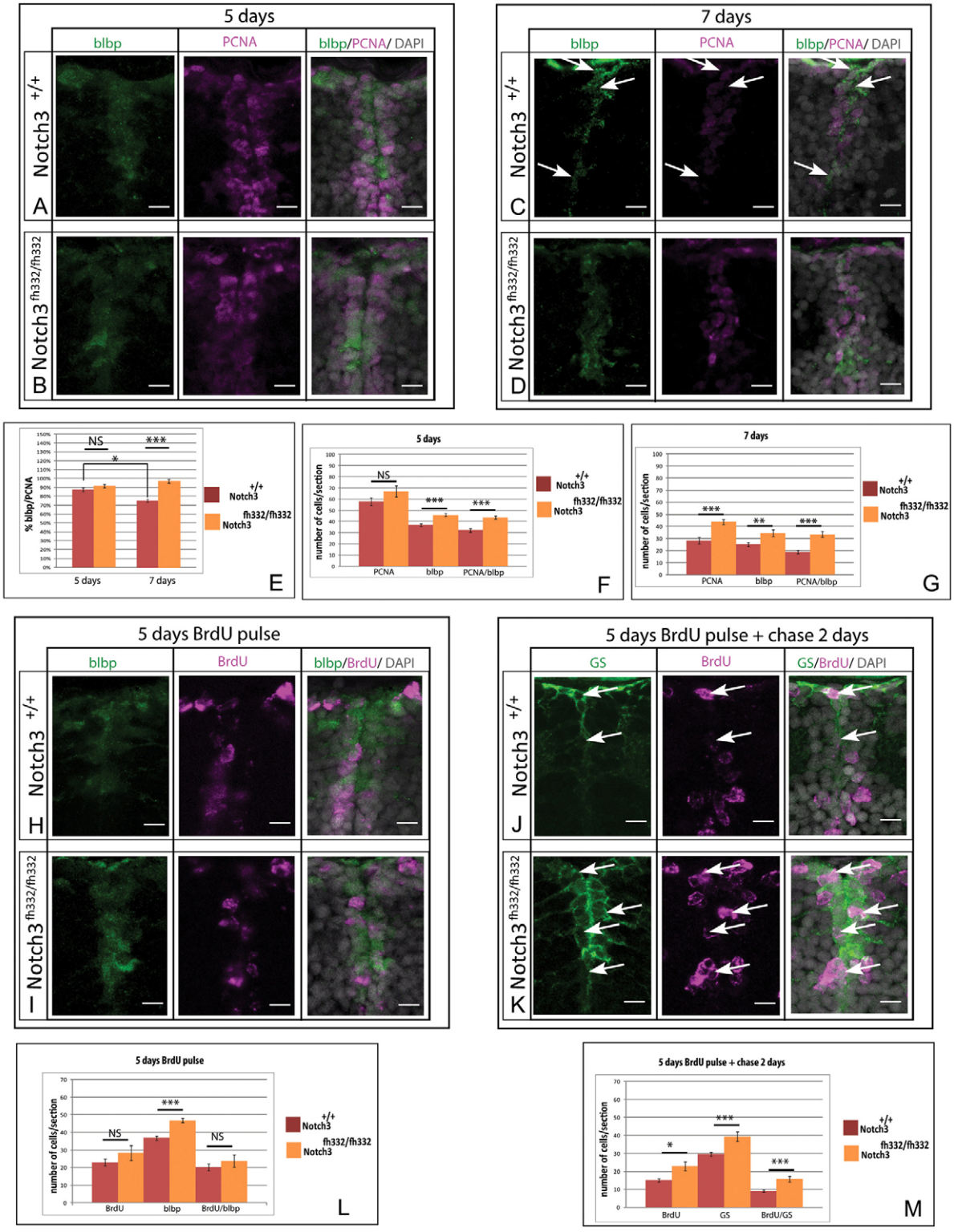

Fig. 7. Notch3 promotes NSC quiescence and limits amplifying divisions in the juvenile pallium. (**A-D**) Cross-sections of the pallial ventricular zone at 5 (C,D) and 7 (A,B) dpf stained for the RG marker BLBP (green) and the proliferation marker PCNA (magenta) (gray: DAPI) in *notch3*$^{fh332/fh332}$ homozygous mutants (B,D) and *notch3*$^{+/+}$ siblings (A,C). White arrows at 7 dpf indicate quiescent RG. (**E-G**) Total number of proliferating cells (PCNA), RG (BLBP) and proliferating RG (PCNA/BLBP) per section at 7 dpf (E) and 5 dpf (F), and proportion of proliferating RG (G). (**H-K**) Cross-sections of the pallial ventricular zone at 5 (H,I) and 7 (J,K) dpf stained for the RG markers BLBP or GS (green) and for BrdU (magenta) (gray: DAPI) in *notch3*$^{fh332/fh332}$ homozygous mutants (I,K) and *notch3*$^{+/+}$ siblings (H,J). 7 dpf animals were pulsed with BrdU at 5 dpf and chased for 2 days. White arrows indicate BrdU-positive cells that remain as RG in mutants. (**L**,**M**) Total number of BrdU-positive cells (BrdU), RG (BLBP or GS) and BrdU-positive RG (BrdU/BLBP or BrdU/GS) per section at 5 dpf immediately after the BrdU pulse (L) and after 2 days of chase (M). **P*<0.05; ***P*<0.005; ****P*<0.0001 (*n*=3 for both *notch3*$^{+/+}$ and *notch3*$^{fh332/fh332}$ fish). Scale bars: 10 µm. Confocal projection images from four optical planes, each 1 µm thick.

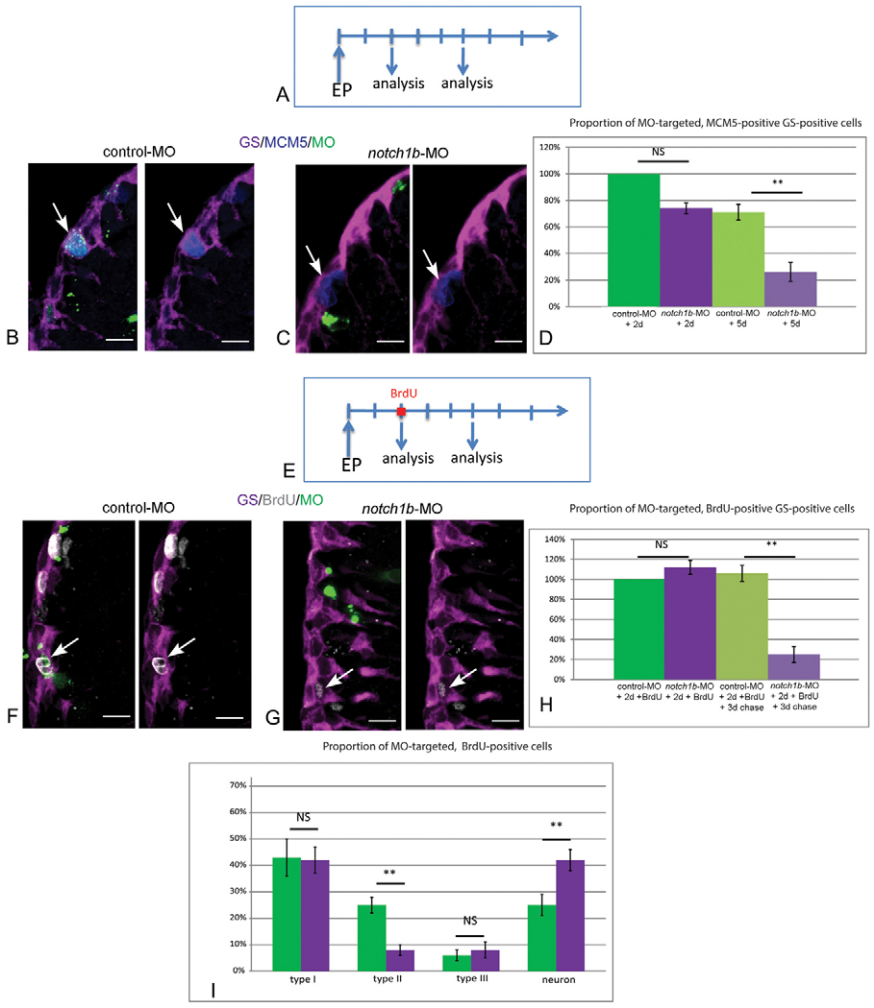

Fig. 8. Notch1b is required for the maintenance of progenitor division and fate. (**A**) Schematic of the *notch1b*-MO knock-down experiment: brains are analyzed 2 and 5 days after electroporation of fluorescein-labeled *notch1b*-MO or control-MO in pallial ventricular cells. (**B**,**C**) Analysis of the proliferation status (anti-MCM5) (blue) of electroporated (fluorescein-positive) (green) RG (anti-GS) (magenta), assessed by immunocytochemistry 5 days after electroporation. Arrows indicate proliferating RG, usually *notch1b*-MO-negative. (**D**) Proportion of MCM5-positive, GS-positive cells within the MO-targeted population, 2 days (P=0.05) and 5 days (**P<0.001) after electroporation (n=3 brains for each condition). (**E**) Schematic of the fate analysis in *notch1b*-MO knock-down experiments: a BrdU pulse is applied 2 days after electroporation of fluorescein-labeled notch1b-MO or control-MO in pallial ventricular cells. Brains are analyzed immediately or after a 3-day chase. (**F**,**G**) Analysis of BrdU labeling (white) in electroporated (fluorescein-positive) (green, arrows) RG (anti-GS) (magenta), assessed by immunocytochemistry after a 3-day chase. Arrows indicate fluorescein-labeled BrdU-positive cells in control-MO (glial cells F) and in *notch1b*-MO (G). (**H**) Proportion of BrdU-positive, GS-positive cells within the MO-targeted population, 2 days (P=0.05) and 5 days (**P<0.001) after electroporation (n=3 brains for each condition). (**I**) Proportion of type I (GS positive, MCM5 negative), type II (GS positive, MCM5 positive), type III (GS negative, MCM5 positive) and non-progenitor cells (GS negative, MCM5 negative) [presumably neurons, which virtually constitute the only non-progenitor cell type generated from the pallial GZ (Chapouton et al., 2010; Rothenaigner et al., 2011)] within the BrdU-positive MO-targeted population 5 days after electroporation (type II, neurons: **P<0.001) (n=3 brains for each condition). Scale bars: 10 μm. Confocal projection images from four optical planes, each 0.5 μm thick.

proliferation parameters of RG cells are not modified at that point and that BrdU incorporation can be used to trace a comparable proportion of type II cells in control and *notch1b*-depleted animals. Following a 3-day chase, the proportion of BrdU-positive cells within the RG population was significantly decreased in *notch1b*-MO compared with control-MO cells (Fig. 8H). Thus, upon Notch1b abrogation, type II RG tend to lose their glial identity. Within the chased BrdU-positive population, the proportion of type III progenitors remained stable in *notch1b*-MO-electroporated cells, but reciprocal shifts affected type II cells and neurons (Fig. 8I). Together, these observations suggest that dividing RG exit the cell cycle upon Notch1b abrogation and that at least some of them prematurely acquire a neuronal fate.

DISCUSSION

The long-term equilibrium of NSC reservoirs in the adult vertebrate brain relies on the tight control of NSC stemness, and several signaling pathways, including Notch, have been implicated in this process. Much less is known on the mechanisms underlying the regulation of NSC activation, in particular towards amplifying NSC divisions, and their impact on the long-term homeostasis of neural GZs. Adult NSCs are endowed with strong quiescence, and we have previously shown that a transient Notch invalidation triggered ventricular proliferation in the adult zebrafish pallium (Chapouton et al., 2010), in the long run increasing all division modes while maintaining their relative proportions (Rothenaigner et al., 2011). Here, combining pharmacological, genetic and morpholino-

mediated invalidations with the tracing of cell divisions and cell fate, we demonstrate that: (1) the control of NSC proliferation by Notch primarily targets cell cycle re-entry from quiescence, and thus NSC activation, and affects symmetrical (but not asymmetrical) RG divisions; (2) long-term pharmacological Notch abrogation results in the sustained activation and a transient amplification of the adult pallial NSC pool, identifying Notch as a protector of homeostasis through the control of NSC quiescence; and (3) Notch3, which is selectively expressed in RG, is the key receptor involved in this process, as its invalidation mimics the effects of a complete abrogation of canonical Notch signaling on RG quiescence and division mode. By contrast, we show that Notch1b, which is expressed in dividing progenitors, is directly or indirectly required for maintaining the progenitor state. The dynamic evolution of the RG proliferation status in the juvenile pallium does not allow us to conclude whether Notch3 gates quiescence exit or rather accelerates quiescence entry. By contrast, the initially quiescent state of most adult RG clearly highlights that Notch3 at this stage limits quiescence exit. In adult, BrdU-tracing experiments monitoring quiescence re-entry upon division also fail to support a model where Notch would accelerate quiescence entry (not shown). Together, our results identify Notch3 as the Notch receptor that limits NSC activation towards amplifying divisions, thereby acting as a major checkpoint for adult GZ homeostasis. The role of Notch3 that we unravel here for the first time in mature NSC pools of the adult vertebrate brain is very reminiscent of the demonstrated function of Notch3 in controlling the quiescence of muscle satellite stem cells, highlighting the general relevance of our conclusions: *Notch3*-deficient mice, although with normal muscle morphology, display an enlarged satellite cell pool with an increased proportion of activated satellite cells (Kitamoto and Hanaoka, 2010). Furthermore, the stimulation of this pool through injury leads to its abnormal amplification in *Notch3*$^{-/-}$ mice, suggesting the exaggerated occurrence of amplifying divisions (Kitamoto and Hanaoka, 2010). Based on these results and ours, we propose that Notch3 is a crucial regulator of stem cell pool size under physiological conditions in adult germinal populations, through limiting stem cell activation towards amplifying divisions.

It remains to be shown whether a similar Notch3-mediated mechanism operates in the mammalian brain, but several observations support this conclusion. Although the mammalian SEZ/SGZ and the zebrafish medial pallium, analyzed here, are not directly homologous domains (Salas et al., 2006; Mueller et al., 2011), their NSCs share fundamental characteristics, such as quiescence, glial attributes and gene expression (Adolf et al., 2006). The fact that Notch receptors other than Notch1 must control adult NSC proliferation/activation was recently hypothesized in the mouse based on the different phenotypes of invalidating RBPJk compared with Notch1 (Basak et al., 2012). The conditional ablation of RBPJk in adult neural progenitors of the SEZ and SGZ led to a transient increase in proliferation of NSCs (Ehm et al., 2010) and, to a larger extent, of the TAP population (Ehm et al., 2010; Imayoshi et al., 2010). By contrast, the conditional inactivation of Notch1 did not impact the NSC proliferation rate but primarily decreased the maintenance/self-renewal of proliferating NSCs and the amplification of TAPs (Ables et al., 2010; Basak et al., 2012). As we demonstrate here, invalidating Notch1b in zebrafish triggered a loss of activated RG and the generation of neurons. Although we have not specifically analyzed the fate of type III progenitors (considered equivalent to TAPs; März et al., 2010), and we also cannot tell at this point whether Notch1b primarily controls cell division or the progenitor state per se, our results directly parallel the demonstrated function for Notch1 in mouse and reinforce the notion that similar molecular processes control the behavior of zebrafish and mouse adult progenitors. Together, our results and the available mouse data strongly suggest that recruiting NSCs towards neurogenesis involves successive Notch-mediated events that display a differential requirement for Notch receptors: Notch3 is the most upstream in the cascade and controls the initial rate of NSC activation, while Notch1 is involved upon activation to permit division and/or maintain the stem cell/progenitor fate. The zebrafish adult pallial GZ is highly enriched in amplifying NSC divisions (Rothenaigner et al., 2011), making this division mode particularly accessible experimentally, while asymmetrical divisions are rare. Symmetric NSC divisions, although infrequent, can be observed from adult rodent NSCs (Morshead et al., 1998). It will also be important to determine whether a similar selectivity in the division mode favored upon a release from Notch(3)-mediated quiescence operates in this case.

Whether the differential activities of Notch1 and Notch3 in adult NSCs are linked with differences in expression or involve truly distinct signaling outputs remains to be directly assessed. The ectopic expression of Notch1 ICD in pallial RG decreases proliferation, mimicking the expected effect of Notch3 signaling (Chapouton et al., 2010). However, the expression of NICD fragments above physiological conditions may bypass endogenous specificities. In mice, Notch1 and Notch3 appear co-expressed in NSCs (Basak et al., 2012), whereas *notch1b* and *notch3* only partially overlap in NSCs in zebrafish (Fig. 4). However, the lack of antibodies detecting the ICD fragments of zebrafish Notch3 and Notch1b prevented a precise mapping of the activities of both receptors. The sequential implication of Notch3 and Notch1 functions in muscle satellite stem cell recruitment (Conboy and Rando, 2002) involves, at least in part, distinct targets for the two receptors (Kitamoto and Hanaoka, 2010), corroborating previous studies that showed target sequence selectivity for Notch1 and Notch3 signaling (Ong et al., 2006). Threshold levels of Notch signaling were recently observed to control specific cellular outputs in pancreatic progenitors and the regenerating spinal cord in zebrafish (Ninov et al., 2012; Dias et al., 2012), and it is also possible that quantitative differences in the signaling efficiencies of Notch1 and Notch3 encode different cellular responses in adult brain NSCs.

Based on the coinciding expression of *her4.1* and glial markers, it had been proposed that Notch signaling via Her4 was primarily involved in maintaining glial identity in the adult brain (Ganz et al., 2010). Our results highlighting the maintenance of glial markers expression in the *notch3* expression domain upon long-term Notch blockade and in *notch3*^{fh332} mutants argue against this interpretation. Instead, Her4 may be involved in preventing NSC activation as an effector of Notch3. Given the strong expression of *her4* in proliferating RG at juvenile stages, however, it is also possible that another Notch3 target controls NSC activation. Profiling data in cultured fibroblasts identified Hes1 as quiescence factor that could directly antagonize senescence and differentiation programs, and was upregulated by Notch (Coller et al., 2006; Sang et al., 2008; Sang and Coller, 2009). Whether Hes1 also directly impacts proliferation is not known. It will be important to assess directly the response of these different *Hes/her* candidates to *notch3* abrogation, and their individual functions in the control of NSC quiescence.

There is an apparent discrepancy between our observations and the genetic invalidation of RBPJk in mouse: NSC proliferation was transient and NSC pools were eventually depleted in conditional RBPJk knockout mice (Ehm et al., 2010; Imayoshi et al., 2010),

whereas long-term Notch blockade led to GZ amplification in the zebrafish adult pallium (Fig. 2). Prolonged LY treatments were followed by neuronal differentiation of a large proportion of amplified RG; however, a histologically normal GZ made of actively proliferating RG was maintained, with no sign of NSC loss (Fig. 3; supplementary material Figs S4, S5). There are several interpretations to these seemingly divergent mouse and zebrafish phenotypes. NSC depletion in RBPJk mutant mice may result from the exhaustion of NSCs – or their entry into a non-activatable state – following a finite number of divisions, which would be reached prematurely in mutants. Terminating lineages have been reported endogenously in aging mice (Encinas et al., 2011), making this hypothesis possible. Compared with mouse, the zebrafish pallium shows a higher capacity for reactivation for repair, for example (reviewed by Kizil et al., 2012), which may suggest a potential for more NSC divisions. However successive lesions have not been performed to repeatedly challenge the germinal pool, and it is unclear which progenitor subtype and division mode(s) are primarily recruited in repair processes. Alternatively, or in addition, NSC depletion in RBPJk-null mice may result from the defective maintenance of stemness upon division in the absence of Notch1 (Ables et al., 2010; Basak et al., 2012). Our results highlight a similar function for zebrafish Notch1b, the abrogation of which by LY should thus have eventually led to NSC loss, in spite of alleviating the repressing effect of Notch3 on RG activation. We consider it unlikely that LY would preferentially target zebrafish Notch3 over Notch1b: the inhibitory activity of LY proved fully efficient during embryonic neurogenesis (not shown), which largely relies on Notch1 function. A higher stability of N1bICD compared with N3ICD, which could induce a delay in Notch1b abrogation, is also not likely of major relevance here, given that the *notch1b*-MO affected RG within 5 days, while we still observed RG amplification even after 3 weeks of LY treatment (supplementary material Fig. S4). More conceivably, it is possible that our LY treatment allowed sub-threshold Notch signaling to operate, which, combined with the large NSC enrichment of the zebrafish adult pallial GZ, resulted in a net NSC amplification response. In addition, factors other than Notch1b may partially compensate to maintain stemness under LY treatment in zebrafish, and/or the lack of Notch1b and Notch3 in activated RG may trigger a phenotype different from the lack of Notch1b alone. Along these lines, the long-term impact of Notch3 invalidation, notably the effect of this regulation on NSC stemness, remains an important issue that should clarify the link between NSC division rate and stemness maintenance.

In conclusion, we propose that maintaining the homeostasis of constitutively neurogenic NSC pools in the mature brain requires successive Notch-dependent steps, of which the most upstream, NSC activation and cell cycle re-entry, is mediated by Notch3, while the subsequent maintenance of the activated NSC requires Notch1. This molecular mechanism is shared with the activation of muscle satellite stem cells and the physiological maintenance of the satellite stem cell pool size, but not with systems that display high cellular turnover, such as hematopoietic, skin epidermis or intestinal stem cells (reviewed by Perdigoto and Bardin, 2013). The general relevance of this distinction, and the mediators of Notch3 versus Notch1b activities, will be important to identify in future studies.

Acknowledgements
We thank our lab colleagues for their scientific and technical input, and Marion Coolen, Isabelle Foucher, Shauna Katz and Emmanuel Than-Trong for their critical reading of the manuscript. Sébastien Bedu provided expert fish care.

Funding
Work in the L.B.-C. laboratory was funded by the EU projects NeuroXsys [FP7/2007-2013, grant agreement number 223262] and ZF-Health [FP7/2010-2015, grant agreement number 242048); and by the L'Agence Nationale de la Recherche (ANR) [ANR-08-CEX-08-000-01 and ANR-2012-BSV4-0004-01], the École des Neurosciences Paris Île de France (ENP) and the La Fondation pour la Recherche Médicale (FRM) [FRP 'Equipe' DEQ20120323692]. The *notch3*^{fh332} mutant allele was generated with the support of the National Institutes of Health [R01 HG002995 to C.B.M.]. Deposited in PMC for release after 12 months.

Competing interests statement
The authors declare no competing financial interests.

Author contributions
A.A., M.K. and L.B.-C. conceived the study and assembled the manuscript; A.A. and M.K. performed experiments on adults; A.B. performed experiments on juveniles; S.G. analyzed *her4* expression and proliferation in adults; L.P. and C.B.M. generated the *notch3fh332* allele.

Supplementary material
Supplementary material available online at
http://dev.biologists.org/lookup/suppl/doi:10.1242/dev.095018/-/DC1

References

Ables, J. L., Decarolis, N. A., Johnson, M. A., Rivera, P. D., Gao, Z., Cooper, D. C., Radtke, F., Hsieh, J. and Eisch, A. J. (2010). Notch1 is required for maintenance of the reservoir of adult hippocampal stem cells. *J. Neurosci.* **30**, 10484-10492.

Ables, J. L., Breunig, J. J., Eisch, A. J. and Rakic, P. (2011). Not(ch) just development: Notch signalling in the adult brain. *Nat. Rev. Neurosci.* **12**, 269-283.

Adolf, B., Chapouton, P., Lam, C. S., Topp, S., Tannhäuser, B., Strähle, U., Götz, M. and Bally-Cuif, L. (2006). Conserved and acquired features of adult neurogenesis in the zebrafish telencephalon. *Dev. Biol.* **295**, 278-293.

Andreu-Agulló, C., Morante-Redolat, J. M., Delgado, A. C. and Fariñas, I. (2009). Vascular niche factor PEDF modulates Notch-dependent stemness in the adult subependymal zone. *Nat. Neurosci.* **12**, 1514-1523.

Basak, O., Giachino, C., Fiorini, E., Macdonald, H. R. and Taylor, V. (2012). Neurogenic subventricular zone stem/progenitor cells are Notch1-dependent in their active but not quiescent state. *J. Neurosci.* **32**, 5654-5666.

Bernardos, R. L. and Raymond, P. A. (2006). GFAP transgenic zebrafish. *Gene Expr. Patterns* **6**, 1007-1013.

Bonaguidi, M. A., Wheeler, M. A., Shapiro, J. S., Stadel, R. P., Sun, G. J., Ming, G. L. and Song, H. (2011). In vivo clonal analysis reveals self-renewing and multipotent adult neural stem cell characteristics. *Cell* **145**, 1142-1155.

Breunig, J. J., Silbereis, J., Vaccarino, F. M., Sestan, N. and Rakic, P. (2007). Notch regulates cell fate and dendrite morphology of newborn neurons in the postnatal dentate gyrus. *Proc. Natl. Acad. Sci. USA* **104**, 20558-20563.

Chapouton, P., Jagasia, R. and Bally-Cuif, L. (2007). Adult neurogenesis in non-mammalian vertebrates. *Bioessays* **29**, 745-757.

Chapouton, P., Skupien, P., Hesl, B., Coolen, M., Moore, J. C., Madelaine, R., Kremmer, E., Faus-Kessler, T., Blader, P., Lawson, N. D. et al. (2010). Notch activity levels control the balance between quiescence and recruitment of adult neural stem cells. *J. Neurosci.* **30**, 7961-7974.

Chapouton, P., Webb, K. J., Stigloher, C., Alunni, A., Adolf, B., Hesl, B., Topp, S., Kremmer, E. and Bally-Cuif, L. (2011). Expression of hairy/enhancer of split genes in neural progenitors and neurogenesis domains of the adult zebrafish brain. *J. Comp. Neurol.* **519**, 1748-1769.

Coller, H. A., Sang, L. and Roberts, J. M. (2006). A new description of cellular quiescence. *PLoS Biol.* **4**, e83.

Conboy, I. M. and Rando, T. A. (2002). The regulation of Notch signaling controls satellite cell activation and cell fate determination in postnatal myogenesis. *Dev. Cell* **3**, 397-409.

Costa, M. R., Ortega, F., Brill, M. S., Beckervordersandforth, R., Petrone, C., Schroeder, T., Götz, M. and Berninger, B. (2011). Continuous live imaging of adult neural stem cell division and lineage progression in vitro. *Development* **138**, 1057-1068.

Dias, T. B., Yang, Y. J., Ogai, K., Becker, T. and Becker, C. G. (2012). Notch signaling controls generation of motor neurons in the lesioned spinal cord of adult zebrafish. *J. Neurosci.* **32**, 3245-3252.

Doetsch, F., García-Verdugo, J. M. and Alvarez-Buylla, A. (1999). Regeneration of a germinal layer in the adult mammalian brain. *Proc. Natl. Acad. Sci. USA* **96**, 11619-11624.

Dong, Z., Yang, N., Yeo, S. Y., Chitnis, A. and Guo, S. (2012). Intralineage directional Notch signaling regulates self-renewal and differentiation of asymmetrically dividing radial glia. *Neuron* **74**, 65-78.

Draper, B. W., McCallum, C. M., Stout, J. L., Slade, A. J. and Moens, C. B. (2004). A high-throughput method for identifying N-ethyl-N-nitrosourea (ENU)-induced point mutations in zebrafish. *Methods Cell Biol.* **77**, 91-112.
Ehm, O., Göritz, C., Covic, M., Schäffner, I., Schwarz, T. J., Karaca, E., Kempkes, B., Kremmer, E., Pfrieger, F. W., Espinosa, L. et al. (2010). RBPJkappa-dependent signaling is essential for long-term maintenance of neural stem cells in the adult hippocampus. *J. Neurosci.* **30**, 13794-13807.
Encinas, J. M., Michurina, T. V., Peunova, N., Park, J. H., Tordo, J., Peterson, D. A., Fishell, G., Koulakov, A. and Enikolopov, G. (2011). Division-coupled astrocytic differentiation and age-related depletion of neural stem cells in the adult hippocampus. *Cell Stem Cell* **8**, 566-579.
Fauq, A. H., Simpson, K., Maharvi, G. M., Golde, T. and Das, P. (2007). A multigram chemical synthesis of the gamma-secretase inhibitor LY411575 and its diastereoisomers. *Bioorg. Med. Chem. Lett.* **17**, 6392-6395.
Folgueira, M., Bayley, P., Navratilova, P., Becker, T. S., Wilson, S. W. and Clarke, J. D. (2012). Morphogenesis underlying the development of the everted teleost telencephalon. *Neural Dev.* **7**, 32.
Ganz, J., Kaslin, J., Hochmann, S., Freudenreich, D. and Brand, M. (2010). Heterogeneity and Fgf dependence of adult neural progenitors in the zebrafish telencephalon. *Glia* **58**, 1345-1363.
Imayoshi, I., Sakamoto, M., Yamaguchi, M., Mori, K. and Kageyama, R. (2010). Essential roles of Notch signaling in maintenance of neural stem cells in developing and adult brains. *J. Neurosci.* **30**, 3489-3498.
Kaslin, J., Ganz, J. and Brand, M. (2008). Proliferation, neurogenesis and regeneration in the non-mammalian vertebrate brain. *Philos. Trans. R. Soc. B.* **363**, 101-122.
Kazanis, I., Lathia, J. D., Vadakkan, T. J., Raborn, E., Wan, R., Mughal, M. R., Eckley, D. M., Sasaki, T., Patton, B., Mattson, M. P. et al. (2010). Quiescence and activation of stem and precursor cell populations in the subependymal zone of the mammalian brain are associated with distinct cellular and extracellular matrix signals. *J. Neurosci.* **30**, 9771-9781.
Kitamoto, T. and Hanaoka, K. (2010). Notch3 null mutation in mice causes muscle hyperplasia by repetitive muscle regeneration. *Stem Cells* **28**, 2205-2216.
Kizil, C., Kaslin, J., Kroehne, V. and Brand, M. (2012). Adult neurogenesis and brain regeneration in zebrafish. *Dev. Neurobiol.* **72**, 429-461.
Kriegstein, A. and Alvarez-Buylla, A. (2009). The glial nature of embryonic and adult neural stem cells. *Annu. Rev. Neurosci.* **32**, 149-184.
Lindsey, B. W. and Tropepe, V. (2006). A comparative framework for understanding the biological principles of adult neurogenesis. *Prog. Neurobiol.* **80**, 281-307.
Louvi, A. and Artavanis-Tsakonas, S. (2006). Notch signalling in vertebrate neural development. *Nat. Rev. Neurosci.* **7**, 93-102.
Lugert, S., Basak, O., Knuckles, P., Haussler, U., Fabel, K., Götz, M., Haas, C. A., Kempermann, G., Taylor, V. and Giachino, C. (2010). Quiescent and active hippocampal neural stem cells with distinct morphologies respond selectively to physiological and pathological stimuli and aging. *Cell Stem Cell* **6**, 445-456.
Ma, M. and Jiang, Y. J. (2007). Jagged2a-notch signaling mediates cell fate choice in the zebrafish pronephric duct. *PLoS Genet.* **3**, e18.
März, M., Chapouton, P., Diotel, N., Vaillant, C., Hesl, B., Takamiya, M., Lam, C. S., Kah, O., Bally-Cuif, L. and Strähle, U. (2010). Heterogeneity in progenitor cell subtypes in the ventricular zone of the zebrafish adult telencephalon. *Glia* **58**, 870-888.
Milan, D. J., Giokas, A. C., Serluca, F. C., Peterson, R. T. and MacRae, C. A. (2006). Notch1b and neuregulin are required for specification of central cardiac conduction tissue. *Development* **133**, 1125-1132.
Mira, H., Andreu, Z., Suh, H., Lie, D. C., Jessberger, S., Consiglio, A., San Emeterio, J., Hortigüela, R., Marqués-Torrejón, M. A., Nakashima, K. et al. (2010). Signaling through BMPR-IA regulates quiescence and long-term activity of neural stem cells in the adult hippocampus. *Cell Stem Cell* **7**, 78-89.
Morshead, C. M., Craig, C. G. and van der Kooy, D. (1998). In vivo clonal analyses reveal the properties of endogenous neural stem cell proliferation in the adult mammalian forebrain. *Development* **125**, 2251-2261.
Mueller, T., Dong, Z., Berberoglu, M. A. and Guo, S. (2011). The dorsal pallium in zebrafish, Danio rerio (Cyprinidae, Teleostei). *Brain Res.* **1381**, 95-105.
Ninov, N., Borius, M. and Stainier, D. Y. (2012). Different levels of Notch signaling regulate quiescence, renewal and differentiation in pancreatic endocrine progenitors. *Development* **139**, 1557-1567.
Ong, C. T., Cheng, H. T., Chang, L. W., Ohtsuka, T., Kageyama, R., Stormo, G. D. and Kopan, R. (2006). Target selectivity of vertebrate notch proteins. Collaboration between discrete domains and CSL-binding site architecture determines activation probability. *J. Biol. Chem.* **281**, 5106-5119.
Perdigoto, C. N. and Bardin, A. J. (2013). Sending the right signal: Notch and stem cells. *Biochim. Biophys. Acta* **1830**, 2307-2322.
Pierfelice, T., Alberi, L. and Gaiano, N. (2011). Notch in the vertebrate nervous system: an old dog with new tricks. *Neuron* **69**, 840-855.
Rothenaigner, I., Krecsmarik, M., Hayes, J. A., Bahn, B., Lepier, A., Fortin, G., Götz, M., Jagasia, R. and Bally-Cuif, L. (2011). Clonal analysis by distinct viral vectors identifies bona fide neural stem cells in the adult zebrafish telencephalon and characterizes their division properties and fate. *Development* **138**, 1459-1469.
Ryu, S., Holzschuh, J., Erhardt, S., Ettl, A. K. and Driever, W. (2005). Depletion of minichromosome maintenance protein 5 in the zebrafish retina causes cell-cycle defect and apoptosis. *Proc. Natl. Acad. Sci. USA* **102**, 18467-18472.
Salas, C., Broglio, C., Durán, E., Gómez, A., Ocaña, F. M., Jiménez-Moya, F. and Rodríguez, F. (2006). Neuropsychology of learning and memory in teleost fish. *Zebrafish* **3**, 157-171.
Sang, L. and Coller, H. A. (2009). Fear of commitment: Hes1 protects quiescent fibroblasts from irreversible cellular fates. *Cell Cycle* **8**, 2161-2167.
Sang, L., Coller, H. A. and Roberts, J. M. (2008). Control of the reversibility of cellular quiescence by the transcriptional repressor HES1. *Science* **321**, 1095-1100.
Seri, B., García-Verdugo, J. M., McEwen, B. S. and Alvarez-Buylla, A. (2001). Astrocytes give rise to new neurons in the adult mammalian hippocampus. *J. Neurosci.* **21**, 7153-7160.
Suh, H., Consiglio, A., Ray, J., Sawai, T., D'Amour, K. A. and Gage, F. H. (2007). In vivo fate analysis reveals the multipotent and self-renewal capacities of Sox2+ neural stem cells in the adult hippocampus. *Cell Stem Cell* **1**, 515-528.
Takke, C., Dornseifer, P., v Weizsäcker, E. and Campos-Ortega, J. A. (1999). her4, a zebrafish homologue of the Drosophila neurogenic gene E(spl), is a target of NOTCH signalling. *Development* **126**, 1811-1821.
Yoon, K. and Gaiano, N. (2005). Notch signaling in the mammalian central nervous system: insights from mouse mutants. *Nat. Neurosci.* **8**, 709-715.